INORGANIC CHEMISTRY

FRONTIERS

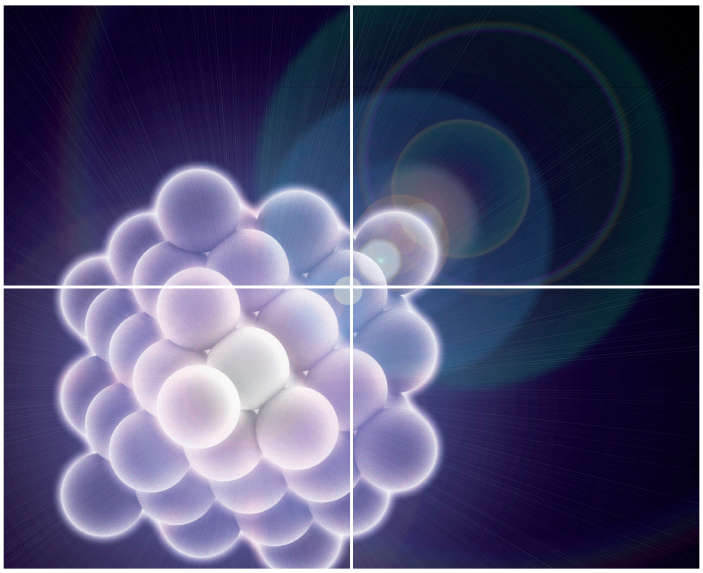

Accepted Manuscript

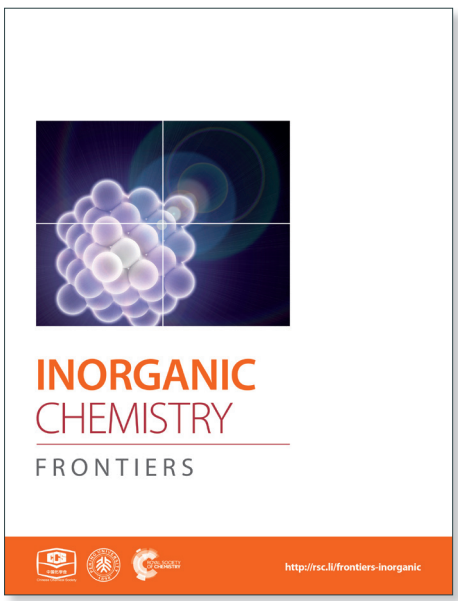

This is an *Accepted Manuscript*, which has been through the Royal Society of Chemistry peer review process and has been accepted for publication.

Accepted Manuscripts are published online shortly after acceptance, before technical editing, formatting and proof reading. Using this free service, authors can make their results available to the community, in citable form, before we publish the edited article. We will replace this *Accepted Manuscript* with the edited and formatted *Advance Article* as soon as it is available.

You can find more information about *Accepted Manuscripts* in the **Information for Authors**.

Please note that technical editing may introduce minor changes to the text and/or graphics, which may alter content. The journal's standard **Terms & Conditions** and the **Ethical guidelines** still apply. In no event shall the Royal Society of Chemistry be held responsible for any errors or omissions in this *Accepted Manuscript* or any consequences arising from the use of any information it contains.

Journal Name

RSCPublishing

ARTICLE

The Slow Magnetic Relaxation Regulated by Ligand Conformation of A Lanthanide Single-Ion Magnet [HexN][Dy(DBM)$_4$]

Cite this: DOI: 10.1039/x0xx00000x

Received 00th January 2012,
Accepted 00th January 2012

DOI: 10.1039/x0xx00000x

www.rsc.org/

Wen-Bin Sun,[a, b] Bing Yan,[a] Yi-Quan Zhang,[a] Bing-Wu Wang,*[a] Zhe-Ming Wang,[a] Jun-Hua Jia[a] and Song Gao*[a]

A mononuclear Dysprosium(III) complex [Hex$_4$N][Dy(DBM)$_4$] (**1**) was synthesized using dibenzoylmethane (DBM) anion ligand with a tetrahexylammonium (Hex$_4$N$^+$) cation balancing the charge. Complex **1** was structurally and magnetically characterized. The local geometry of Dy(III) ions is close to the ideal D_{4d} symmetry. The temperature and frequency-dependent out-of-phase ac susceptibility peaks were observed in the absence of a static dc field. The relaxation energy barrier U_{eff} = 27.7 K and τ_0= 1.3×10^{-7} s were obtained by Arrhenius fitting. It is interesting that the quantum tunneling of magnetization was suppressed when two optimum dc fields (300 and 1500 Oe) were applied, two distinct thermal relaxation processes were observed with U_{eff} = 56.6 K, τ_0 = 6.6×10^{-10} s for 300 Oe and U_{eff} = 68.1 K, τ_0 = 3.4×10^{-11} s and U_{eff} = 88.0 K, τ_0 = 5.0×10^{-10} s for 1500 Oe, respectively. The two thermal relaxation processes were also recognized clearly under zero dc field for the analogue with 20 times magnetic site dilution by Y(III). Nevertheless there is only one crystallographically independent Dy(III) ion in this system. Further inspection to the crystallographic structure reveals that the benzene disorder within the conjugated system of the *β*-diketonate ligand could change the delocalized electron distribution on the carbonyl coordination oxygen atoms and resulted in small different ligand fields, which account for the multiple relaxation processes. *Ab initio* calculations confirm the two energy barriers derived from two disorder structures.

Introduction

The single-molecule magnets (SMMs) are attracting the increasing interest due to their potential applications in high density information storage, quantum computing, spintronics device[1-6] and magnetic refrigeration.[7] Transition metal clusters once dominated this investigation field since the archetype Mn_{12}-acetate SMMs, in which possessing a large spin ground state (*S*) in combination with a large uniaxial (or Ising-type) magnetic anisotropy (*D*) leads to an anisotropic energy barrier (U_{eff}) to block the magnetization reversal.[8-11] In recent years, however, there has been a growing trend that enhancing magnetic anisotropy rather than ever-larger spins may be a more effective strategy to increase U_{eff} and blocking temperature (T_B).[12, 13] The lanthanide-containing SMMs are widely studied due to the strong spin-orbit coupling and the significant magnetic anisotropy. Up to now, there is a number of lanthanide SMMs, involving *d*-*f* and pure *f*-based polynuclear SMMs,[14-18] are developed and exhibit significant SMM behavior with higher U_{eff} and T_B compared to transition metal SMMs.[19-21] Meawhile, the pure mononuclear 4*f* and 5*f*-based SMMs as well as mononuclear transition (3*d*) metal, also named single-ion magnet (SIM), appeared as a kind of promising SMMs in recent years.[22-28] The relative simple geometry structure of SIMs provides the facility to study and understand the relationship between the structure and the magnetic properties. From the point of view of ligand field theory, to date, the local symmetry of lanthanide ions in many of the known examples of SIMs reported so far could be regard approximately as a square antiprismatic (SAP). That has steered our efforts to achieve high magnetic axiality *via* designing the local environment of lanthanide ions and tuning the anisotropy of SMM systems. However, the relationship between the geometry structure and relaxation barrier was not clear for most of lanthanide based SIMs. The small change of the coordination environment and ligand field strength may induce the big change of relaxation properties. Unfortunately, it is very difficult to control the tiny change of ligand field around the metal ion by ligand modification for the geometry distortion and complicated inter-molecular interactions. The conformation change of ligand may provide a subtle way to deepen our understanding on the magneto-structural correlations of SIMs. In this report, we use a classic organic compound *β*-diketonate dibenzoylmethane (DBM) as ligand to construct an approximate square antiprismatic coordination geometry. This kind of complexes with four *β*-diketonate ligands has been previously investigated for their prominent luminescent properties, but their single-molecule magnetic properties are unexplored.[29] Herein, we demonstrate that the tetrikis(*β*-diketonate) complex [Hex$_4$N][Dy(DBM)$_4$] (**1**) which behaves as

an SIM and represents one of the few examples with well-defined multiple relaxation modes in SIM systems.

Results and discussion

The reaction of 4 equiv of dibenzoylmethane anions dehydrogenized by NaOH with 1 equiv of $DyCl_3$ and 1 equiv of tetrahexylammonium (Hex_4N^+) cation balancing the system in anhydrous ethanol (EtOH) for 4 h, give rise to the mononuclear complex **1** with formula $[Hex_4N][Dy(DBM)_4]$. The collection of the filtrate was recrystallized from 2-butanone to provide fine needles of **1** that crystallizes in the monoclinic space group $P2_1/n$ and contains a complete mononuclear complex in the asymmetric unit. The molecular structure of **1** is depicted in Fig. 1, and pertinent data are summarized in Table 1, 2, in which there are eight O atoms from four DBM ligands coordinating to the central Dy(III) ion. On the top of $[Dy(DBM)_4]^-$ unit, there is a tetrahexylammonium $[Hex_4N]^+$ cation to balance the system charge and results in a helicopter-like structure. The center Dy(III) ion coordinated by eight Oxygen forms an approximate square antiprismatic (SAP) geometry. The shortest inter-molecular Dy…Dy distance is 10.7370 Å. There exists the partial disorder of the carbon atoms from the cation alkyl chain and benzene rings although the crystal data were collected under 123 K (Fig. S1).

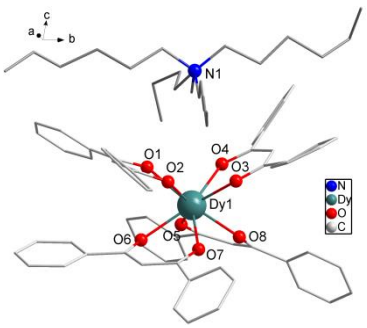

Fig. 1 Partially labelled molecular structure of [Hex4N][Dy(DBM)4], **1**. Colour code: Dy (teal), O (red), N (blue) C (grey). H atoms and disorder atoms were omitted for clarity.

As shown in Fig. 1 and Fig. S1, four O atoms from two DBM ligands compose an upper and a lower square of SAP defined by the mean planes through the coordinating oxygen atoms (O1, O2, O3, O4 and O5, O6, O7, O8) and each moiety is twisted with the smallest 44.42° with respect to the other. This angle is very close to that expected for an ideal D_{4d} symmetry (ϕ = 45°). The average distance between the four neighboring oxygen atoms d_{in} is 2.7805 Å and the interplanar distance (d_{pp}) is 2.5830 Å between the upper and lower planes. The two planes are in a nearly parallel arrangement with a slight tilt angle of 1.09°. The ratio d_{in}/d_{pp} is indicative of an axial distortion (elongation or compression) of the square antiprism around the Dy(III) ions (Fig. S1). As for the first two 4*f*-based SIMs,[22, 23] both of which possessed a pseudo-D_{4d} symmetry, the different distortion of the antiprismatic site, axially compressing for $[Er(W_5O_{18})_2]^{9-}$ and axially elongating for the $[TbPc_2]^-$, which leads to a different splitting of the $\pm M_J$ levels of 4f electrons. For the SIM species, the ligand field may play a crucial role in determining the anisotropy of the paramagnetic ion center. The analysis using the method of Continuous Shape Measures (CShMs)[30,31] gives the deviation parameter *P* of 0.287 for D_{4d} symmetry and $[TbPc_2]^-$ [23b] system gives *P* of 1.307. In this case, the small *P* value in consistent with the d_{in}/d_{pp} value 1.076 closing to 1 representing the ideal square antiprismatic geometry. It indicates that the coordination geometry surrounding the Dy(III) center is close to the ideal D_{4d} symmetry. This geometrical deviation from ideal D_{4d} symmetry in the crystal field, although small, seems to be sufficient to induce the completely change of magnetic relaxation properties of these 4*f*-based SIMs.

Magnetic measurements were performed on polycrystalline samples of **1** using Quantum-Design MPMS and PPMS magnetometers. The temperature dependence of the magnetic susceptibility $\chi_M T$ for **1** is shown in Fig. 2. The value of $\chi_M T$ is 14.18 cm^3Kmol^{-1} at 300 K, which is in good agreement with the theoretical value for one isolated Dy(III) ion (S = 5/2, L = 5, $^6H_{15/2}$, g = 4/3). On lowering the temperature, the $\chi_M T$ product decreases gradually and more rapidly below 50 K, which is likely due to crystal-field effects (*i.e.* thermal depopulation of the Ln(III) Stark sublevels) and/or the possible antiferromagnetic dipole-dipole interaction between the molecules. On the other hand, the plateau of $\chi_M T$ value around 10.8 cm^3Kmol^{-1} at the low temperature is observed, suggesting negligible magnetic interactions.

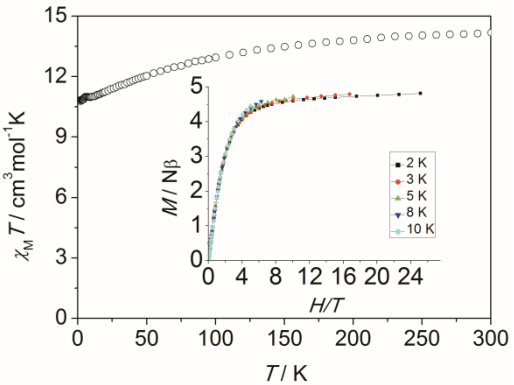

Fig. 2 Temperature dependence of $\chi_M T$ measured at 1 kOe for **1**, (inset: experimental *M vs. H/T* plots at different temperatures 2, 3, 5, 8, and 10 K).

The magnetization of **1** under zero to 50 kOe dc field at 2, 3 5, 8 and 10 K are shown in Fig. S2. The corresponding maximum value of 4.8 *N*β and the lack of saturation of magnetization at 50 kOe can be attributed to crystal-field effects and the low lying excited states. The non-superposition of the *M vs. H/T* plots at higher field (inset, Fig. 2) indicates the presence of significant magnetic anisotropy. In addition, it is worth mentioning that the *M vs H* data do not exhibit a hysteresis at 1.8 K with the sweep rate used in a traditional SQUID magnetometer (100-300 Oe min^{-1}), while it could be observed when a 50 Oe s^{-1} sweep rate was used in a Quantum Design PPMS magnetometer on polycrystalline sample, *vide infra* (Fig. S3).

To probe the magnetic dynamic behavior of **1**, the alternating-current (ac) susceptibilities at various frequencies and temperatures under the absence of dc field were measured and depicted in Fig. 3 and Fig. S4. Both in-phase (χ') and out-of-phase (χ'') susceptibilities show the frequency dependence behavior, which clearly indicates the slow relaxation of magnetization of **1**. The peaks can only be observed at frequencies higher than 3160 Hz, and a broad slope between 5.5 and 10 K can be also found, as well as a tail of the peak below 4 K. The former slope is likely indicative of the existence of another relaxation process whereas the latter tails could be attributed to the quantum tunneling of magnetization (QTM) at

a zero dc field. The QTM process was also found in some other lanthanide-containing SMMs.

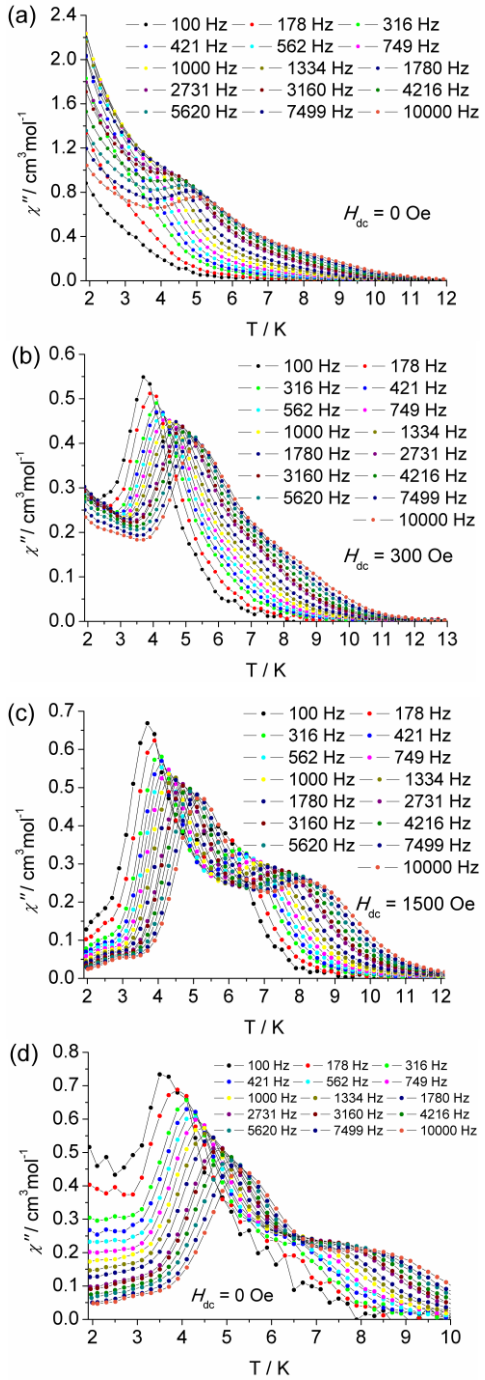

Fig. 3 The temperature dependence of ac susceptibility at indicated frequencies for complex **1** under zero (a), 300 Oe (b), 1500 Oe (c) dc field and for diluted sample under zero dc field (d).

In the frequency dependent susceptibilities measurement, the temperature independent peaks at the low temperature range were observed (Fig. S6), which further proved the occurrence of resonant QTM process. Usually, an optimum dc field could be used to suppress the QTM process, since it could lift the degeneracy of the $\pm M_J$ energy levels and reduce the probability of the zero-field QTM between the two states. The optimum field was selected by determining which field was able to slow the frequency dependent χ'' maxima to the slowest relaxation rate. For the low temperature relaxation process centered at 5 K, the optimum field was found to be 300 Oe (Fig. S11, 13). Therefore, the ac susceptibility was measured under this optimum field, as shown in Fig. 3 and Fig. S8. The significant χ'' peaks were detected even at low frequency as 100 Hz. The thermally activated relaxation process was characterized by the frequency dependent χ'' peaks at the temperature range 3.5 (100 Hz) to 5.5 K (10000 Hz). The QTM process overlaps this relaxation in the absence of an external dc field. As mentioned above, there is a broad slope in the temperature range 5.5 to 9.5 K, which is most likely indicative of another relaxation process. To confirm another process possibly being prominent in high temperature regime, a similar selection of optimum external dc field was performed at 6.5 K. An optimum 1500 Oe external dc field was extracted (Fig. S12, 13). Thus the ac susceptibility was measured under 1500 Oe dc field, as shown in Fig. 3. As expected, the second relaxation process is unequivocally detected from 5.5 K (100 Hz) to 8 K (10000 Hz). The two thermally activated regimes are also confirmed by the measurement of frequency dependent χ'' (Fig. S9). In which, two distinct frequency dependent regions with ac susceptibility peaks are detected relating to the low temperature relaxation (LR) process in 4 K-5.25 K and high temperature relaxation (HR) 6.5 K-9 K.

The multiple relaxation processes have been observed in several reported *f*-based SMMs due to the existence of different anisotropic centers or isomers and conformers in the crystal. Nevertheless, the observation of multiple relaxation process in Dy-based SIM with only one crystallographically independent center was rarely reported.[32-37] The synthesis of SIMs with well-defined multiple relaxation and control of the multiple relaxation pathways are also challenging. However, this type of studies will improve our understanding on such unusual relaxation mechanisms and further provide new clues to enhance the properties of SMMs. Recently, we have reported an organometallic SIM (Cp*ErCOT), displayed two relaxation processes due to the different conformers caused by the disorder of COT group in molecule.[25, 38] There are four other SIMs examples showing multiple relaxations with one single metal center, while few of them have been shown clearly to exhibit well-resolved pathways for slow magnetic relaxation. The source of these multiple pathways is not very clear either. In order to investigate the role of the intermolecular interaction for this unusual SMMs behavior, we repeat the magnetic investigation on a magnetic diluted sample by the isostructural Y(III) analogue with a molecular ratio of 1 : 20 (Fig. S14-S19). The structure of Y(III) analogue has been also confirmed crystallographically (Table S1).

The static magnetic properties are nearly not affected by magnetic dilution (Fig. S14). But the characteristic the χ'' peaks are significantly low-frequency shift. The first peak is observed at 32 Hz (Fig. S15, 16), and there is a shoulder plateau in the temperature range higher than 5 K and frequency larger than 100 Hz. At the higher frequency range from 100 Hz to 10000 Hz, another relaxation process can be recognized clearly in the absence of an external field (Fig. 3 bottom and Fig. S17). Therefore, these two relaxation processes are confirmed to be attributed to the intrinsic properties of the centered Dy(III) ions, which is not induced by an intermolecular interaction. By diluting the samples, the QTM is efficiently suppressed as in the case under an applied external dc fields.

The hysteresis loop, as an important characteristic of magnetic bistability of magnets, was observed on the undiluted polycrystalline sample with a sweep rate 50 Oe s^{-1}. The waist-constricted hysteresis loop is closed at zero field for the undiluted sample, which is associated with the QTM process in the absence of external field. In contrast, the diluted sample displays a small opening loop at zero field for the dipole-dipole interaction is reduced and the QTM process compressed (Fig. S3).

For a thermal assisted Orbach relaxation, magnetic data fitting using the Arrhenius law ($\tau = \tau_0 \exp(U_{eff}/kT)$, Fig. 4) could provide effective relaxation energy barrier of U_{eff} and pre-exponential factor τ_0. The fitting results are collected in Table S1. As for the low temperature relaxation process, the increase of the anisotropic barrier from 27.7 K ($\tau_0 = 1.3\times10^{-7}$ s) at zero dc field to 56.6 ($\tau_0 = 6.6\times10^{-10}$ s) and 68.1 K ($\tau_0 = 3.4\times10^{-11}$ s) after applying 300 and 1500 Oe dc field was observed as usually seen in 4*f*-based SMMs. The relative lower energy barrier and longer τ_0 are indicative of the QTM process dominating and the pre-exponential factors consist with the expected values around 10^{-6}–10^{-11} s for the SMMs system. The estimated energy barrier of high temperature relaxation process is 88.0 K with $\tau_0 = 5.0\times10^{-10}$ s, which is not affected obviously even a 5000 Oe dc field was applied (Fig. S5). The diluted system displays two relaxation process with the barriers of 63.8 K ($\tau_0 = 1.6\times10^{-10}$) for LR and 79.8 K ($\tau_0 = 1.5\times10^{-9}$) for HR. The LR and HR energy barriers and pre-exponential factors are consistent with values under 1500 Oe external dc field. The presence of two relaxation processes was further examined using a graphical representation, χ'' versus χ' (Cole–Cole plot), which showed the evolution from a low temperature relaxation to a high temperature process under 1500 Oe dc field, as well as in the diluted system (Fig. S10).

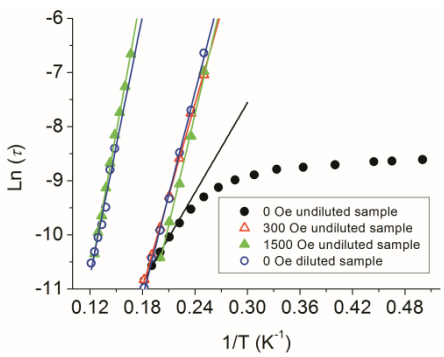

Fig. 4 Plots of ln(τ) vs T^{-1} at H_{dc} = 0, 300 and 1500 Oe for the undiluted and diluted sample (DS). The solid lines represent Arrhenius fits of the frequency-dependent data.

These facts led us to the conclusion that an enlarged intermolecular distances or an applied external dc field can suppress the QTM processes and make the relaxation process (mainly thermally activated one) distinguished. The various diluted concentration or ac frequencies could make the multiple relaxation pathways apparent when lacking of an external dc field. The different magnitude external dc field can also separate the multiple relaxation processes. These phenomena have been sparsely observed except for few actinide (U) [39] and lanthanide-based SIM systems with single geometrical metal center. Nevertheless few of them were successful to separate the multiple processes. The source of these multiple relaxation processes is yet to understand. [34-36]

In our case, the alkyl chain of the counter Hex_4N^+ cation and the benzene ring are partially disordered (see Fig. S1). Particularly the disorder benzene rings in the conjugated system of the *β*-diketonate ligand DBM, although the benzene ring is remote from the Dy(III) center, could disturb the delocalized electron distribution on the carbonyl oxygen atoms, which are in the first coordination sphere of Dy(III) ion and construct the main negative charge density of ligand field. In order to examine if the disorder could change magnetic relaxation, *ab initio* calculations of relaxation barrier were performed on two possible geometry configuration of molecule. The two disorder structures for **1** are labeled as **1**a and **1**b (Fig. S1), for which the magnetic easy axial and corresponding *g* tensors and energy different Δ*E* between ground state and first excited state, which is related to the thermal relaxation energy barriers in lanthanide based SMMs, are listed in Table S2-S4. The calculation results reveal that both disorder structures possess significant uniaxial magnetic anisotropy with relative large g_z value 19.5, while the calculated energy different Δ*E* is distinct with ΔE_{1a} 80 K and ΔE_{1b} 102 K, however the relaxation process with relative lower energy barrier can be cautiously assigned to **1**a conformer because of the larger transverse $g_{X,Y}$ values. Although the calculated energy barriers are slightly higher than the ones from experiments, the difference of 22 K between them is well consist with the difference of U_{eff} 20 K and 16 K for the 1500 Oe and dilution conditions in magnetic measurements. Therefore we proposed the two relaxations processes were attributed to the different disorder coordination environments in **1**. The very recent report about a Dy-based SIM with disorder ligands supports our inference. [37] The role of the second coordination sphere on the magnetic anisotropy was predicted for Co(II) ions. It was also found in a DOTA-Dy SIMs system[40]. In the latter case, the apical coordination water molecule could influence the direction of magnetic axes. The rotation of the water molecule could then affect the relative population of the Dy 5*d* orbitals through a *p* interaction with the oxygen atom. These interesting phenomena of two relaxation processes in one crystallographically independent Dy(III) sites are recently also considered to be related to the condensed phase, *i. e.* that may not be related to the chemical nature of the relaxing centers.[41] Whereas our investigation demonstrates how sensitive the magnetic relaxation of Dy(III) center is to the subtle change in local coordination environment involving the minor distortion possibly caused by the ligand disorder albeit beyond the first coordination sphere.

Experimental Section

All chemicals and solvents were obtained from commercial sources and were used as received, without further purification.

Synthesis of [HexN][Dy(DBM)$_4$] (1)

This was prepared according to the literature[42] procedure with slight modifications. To a solution of dibenzoylmethane (4 mmol, 0.900 g), $DyCl_3\cdot6H_2O$ (1 mmol, 0.389 g) and Hex_4NCl (1 mmol, 0.390 g) in 35 mL of hot ethanol was added 2.0 ml. of 2.0 M sodium hydroxide solution under stirring. A dense off-white microcrystalline precipitate separated immediately. After cooling the mixture, the solid was collected and recrystallized from 2-butanone to give 1.098 g of **1** with 77.9 % yield. Elemental analysis cald for $C_{84}H_{96}DyNO_8$: C, 71.54; H, 6.86; N, 0.99 %. Found: C, 71.45; H, 6.84; N, 1.08. IR (KBr/cm^{-1}): 3415, 1616, 1573, 1522, 1458, 1387, 1309, 1259, 1192, 1136, 671.

The diluted sample was synthesized by the same as that employed for complex **1**, except that $DyCl_3\cdot6H_2O$ (0.05 mmol, 0.0193 g) and $YCl_3\cdot6H_2O$ (1 mmol, 0.3041 g) were employed as

rare-earth salt and the final filtrate was collected and recrystallized from 2-butanone to give 1.1651 g of **1** with 82.27 % yield. The ICP and EA analyses reveal the ratio of Dy(III):Y(III) is 17.2:1. Elemental analysis cald for $C_{84}H_{96}Y_{0.95}Dy_{0.05}NO_8$: C, 75.28; H, 7.22; N, 1.05 %. Found: C, 75.45; H, 7.31; N, 1.10.

Physical measurements

Elemental (C, H and N) analyses (EA) were performed on a Perkin-Elmer 2400 analyzer. Fourier transform IR spectra were measured on a Perkin-Elmer Spectrum One spectrometer with samples prepared as KBr pellets. For the magnetic properties measurement, samples were fixed by eicosane to avoid moving during measurement. The elements Dy and Y were quantitatively analysed by Inductively Coupled Plasma-Atomic Emission Spectrometer (ICP-AES) using a Leeman PROFILE SPEC spectrometer. Direct current susceptibility and alternative current susceptibility measurements were carried out under an oscillating ac field of 3 Oe with frequencies in the range from 1 to 997 Hz and 10 to 10000 Hz were performed on a Quantum Design MPMS XL-5 SQUID and Quantum Design PPMS magnetometer on polycrystalline samples, respectively. Data were corrected for the diamagnetism of the samples using Pascal constants and the sample holder by measurement. The amount of diluted sample used for magnetic measurements had to be doubled with respect to the other measurements in order to obtain a reliable signal from the SQUID magnetometer.

X-ray Crystallography

Data were collected on a Nonius Kappa CCD diffractometer with Mo Kα radiation (λ = 0.71073 Å). Empirical absorption corrections were applied using the Sortav program. All structures were solved by direct methods and refined by full-matrix leastsquares on F2 using the SHELX program[43]. H atoms can be located from the difference Fourier synthesis but added Details of the crystal parameters, data collection and refinements for **1** is summarized in Table 1, 2. CCDC: 902442 and 927860 contain the supplementary crystallographic data for complex **1** and the Y(III)-analogue. This data can be obtained free of charge from the Cambridge Crystallographic Data Centre via www.ccdc.cam.ac.uk/data_request/cif.

Table 1. Crystallographic data for 1

	1	Y- analogue
Empirical formula	$C_{84}H_{96}DyNO_8$	$C_{84}H_{92}YNO_8$
FW (g.mol^{-1})	1410.12	1332.50
Crystal system	monoclinic	monoclinic
Space group	$P2_1/n$	$P2_1/n$
Temperature (K)	123.01(10)	293(2)
a (Å)	16.5109(4)	16.5033(4)
b (Å)	24.3839(9)	24.3631(8)
c (Å)	18.6385(5)	18.6445(4)
α (°)	90	90
β (°)	105.084(3)	105.028
γ (°)	90	90
V (Å^3)	7245.3(4)	7240.1(3)
ρ_{cacd} (Mg.m^{-3})	1.286	1.222
μ (mm^{-1})	1.088	1.576
F(000)	2920	2824
Collected reflections	64668	28791
Independent relections	15740	12750
R_{int}	0.0518	0.0429
R_1 [I > 2σ(I)]	0.0701	0.1042
wR_2 (all data)	0.1338	0.2743
Goodness of fit on F2	1.139	1.043

Table 2. Selected bond bengths (Å) and Angles (o) for 1.

Dy1-O4	2.350(3)	Dy1-O3	2.342(4)
Dy1-O6	2.368(4)	Dy1-O2	2.337(3)
Dy1-O8	2.315(4)	Dy1-O1	2.335(4)
Dy1-O5	2.328(3)	Dy1-O7	2.329(3)
O5-Dy1-O4	77.30(12)	O3-Dy1-O4	71.63(13)
O5-Dy1-O3	140.72(13)	O3-Dy1-O6	143.55(12)
O5-Dy1-O1	80.11(14)	O1-Dy1-O4	79.20(13)
O5-Dy1-O2	146.06(15)	O1-Dy1-O3	115.95(13)
O5-Dy1-O6	73.27(12)	O1-Dy1-O2	71.43(13)
O5-Dy1-O7	115.54(12)	O1-Dy1-O6	75.01(14)
O8-Dy1-O5	71.78(14)	O2-Dy1-O4	113.90(11)
O8-Dy1-O4	77.35(12)	O2-Dy1-O3	70.78(13)
O8-Dy1-O3	78.38(13)	O2-Dy1-O6	81.65(12)
O8-Dy1-O1	146.60(12)	O7-Dy1-O4	143.51(15)
O8-Dy1-O2	140.55(14)	O7-Dy1-O3	79.55(13)
O8-Dy1-O6	112.33(12)	O7-Dy1-O1	134.88(12)
O8-Dy1-O7	75.27(12)	O7-Dy1-O2	75.45(12)
O4-Dy1-O6	143.54(14)	O7-Dy1-O6	70.57(14)

Computational details

The g tensor and fine electronic structure were calculated using CASPT2 method based on preceding CASSCF calculation on the model structure 1a and 1b with MOLCAS 7.8 program package.[44]. The spin-orbit coupling was included by state interactions under the mean-field spin-orbit Hamiltonian with RASSI program. In all calculations, the basis sets are atomic natural orbitals from the MOLCAS ANO-RCC library. The following contractions were used: [8s7p5d4f2g1h] for Dy, [4s3p2d] for O and C, and [2s] for H.

Conclusions

We have presented the structural and magnetic properties for a mononuclear Dy(III) compound $[Hex_4N][Dy(DBM)_4]$ (**1**), which behaves as a new type SIMs. It displays unusual two relaxation processes deriving from the visually only one crystallographically independent center. These two processes are well separated by dilution or applying a gradient enhanced field. In this case, the behaviour of multiple relaxations from single paramagnetic center is an interesting phenomenon, which was tentatively attributed to the different ligand field configuration caused by disorder in the conjugated system of the β-diketonate ligand that generates different magnetic anisotropy. This system provides a synthetic strategy for isolation of lanthanide-based SIMs exclusively encapsuled by simple β-diketonate analogues. This also presents an opportunity to shed light on fine-tuning of the magnetic properties of these SIMs by modifying the encapsulating and balancing ligands, and further to explore the influence of local symmetry and ligand field strength on this relative simply SIM system.

Acknowledgements

This work was supported by the NSFC (21290171, 21321001), BJSFC (2122023) and the National Basic Research Program of China (2010CB934601, 2013CB933401) and Educational Commission of Heilongjiang Province (1254G045, 12541639).

Notes and references

[a] Beijing National Laboratory of Molecular Science State Key Laboratory of Rare Earth Materials Chemistry and Applications, College of Chemistry and Molecular Engineering, Peking University Beijing 100871, China.

[b] Key Laboratory of Functional Inorganic Material Chemistry Ministry of Education, Heilongjiang University, Harbin 150080, China.

† Electronic Supplementary Information (ESI) available: Additional figures and magnetic data and *ab* inito calculations results. CCDC 902442 and 927860 for **1** and Y-analogue. For ESI and crystallographic data in CIF or other electronic format see DOI: 10.1039/b000000x/

1 R. Sessoli, D. Gatteschi, A. Caneschi and M. A. Novak, *Nature*, 1993, **365**, 141.
2 D. Gatteschi, R. Sessoli, J. Villain, *Molecular Nanomagnets*, Oxford University Press, Oxford, 2006.
3 J. van Slageren, *Top. Curr. Chem.* 2012, **321**, 199.
4 D. Gatteschi and R. Sessoli, *Angew. Chem. Int. Ed.* 2003, **42**, 268.
5 L. Bogani and W. Wernsdorfer, *Nat. Mater*. 2008, **7**, 179.
6 R. Vincent, S. Klyatskaya, M. Ruben, W. Wernsdorfer, F. Balestro, *Nature*, 2012, **488**, 357.
7 F. Torres, J. M. Herńandez, X. Bohigas and J. Tejada, *J. Appl. Phys. Lett.* 2000, **77**, 3248.
8 A. Caneschi, D. Gatteschi, R. Sessoli, A. L. Barra, L. C. Brunel, M. Guillot, *J. Am. Chem. Soc*. 1991, **113**, 5873.
9 G. E. Kostakis, A. M. Ako, A. K. Powell, *Chem. Soc. Rev*. 2010, **39**, 2238.
10 M. Murugesu, M. Habrych, W. Wernsdorfer, K. A. Abboud, G. Christou, *J. Am. Chem. Soc.* 2004, **126**, 4766.
11 A. M. Ako, I. J. Hewitt, V. Mereacre, R. Cl_erac, W. Wernsdorfer, C. E. Anson, A. K. Powell, *Angew. Chem. Int. Ed*. 2006, **45**, 4926.
12 E. Ruiz, J. Cirera, K. Cano, S. Alvarez, C. Loosec, K. Kortus, *Chem. Commun.* 2008, 52.
13 J. M. Zadrozny, M. Atanasov, A. M. Bryan, C. Y. Lin, B. D. Rekken, P. P. Power, F. Neese, J. R. Long, *Chem. Sci.* 2013, **4**, 125.
14 S. Osa, T. Kido, N. Matsumoto, N. Re, A. Pochaba, J. Mrozinski, *J. Am. Chem. Soc.* 2004, **126**, 420.
15 J. Tang, I. Hewitt, N. T. Madhu, G. Chastanet, W. Wernsdorfer, C. E. Anson, C. Benelli, R. Sessoli, A. K. Powell, *Angew. Chem. Int. Ed.* 2006, **45**, 1729.
16 D. P. Mills, F. Moro, J. McMaster, J. van Slageren, W. Lewis, A. J. Blake, S. T. Liddle, *Nat. Chem.* 2011, **3**, 454.
17 P.-H. Lin, T. J. Burchell, L. Ungur, L. F. Chibotaru, W. Wernsdorfer, M. Murugesu, *Angew. Chem. Int. Ed.* 2009, **48**, 9489.
18 B. W. Wang, S. D. Jiang, X. T. Wang, S. Gao, *Sci China Ser B-Chem*, 2009, **52**, 1739-1758.
19 R. J. Blagg, C. A. Muryn, E. J. L. McInnes, F. Tuna, R. E. P. Winpenny, *Angew. Chem. Int. Ed.* 2011, **50**, 6530.
20 J. D. Rinehart, M. Fang, W. J. Evans, J. R. Long, *Nat. Chem.* 2011, **3**, 538.
21 J. D. Rinehart, M. Fang, W. J. Evans, J. R. Long, *J. Am. Chem. Soc.* 2011, **133**, 14236.
22 (a) N. Ishikawa, M. Sugita, T. Ishikawa, S.-Y. Koshihara, Y. Kaizu, *J. Am. Chem. Soc*. 2003, **125**, 8694; (b) F. Branzoli, P. Carretta, M. Filibian, G. Zoppellaro, M. J. Graf, J. R. Galan-Mascaros, O. Fuhr, S. Brink, M. Ruben, *J. Am. Chem. Soc.* 2009, **131**, 4387.
23 (a) M. A. AlDamen, J. Clemente Juan, E. Coronado, C. Martí-Gastaldo, A. Gaita-Ariño, *J. Am. Chem. Soc*. 2008, **130**, 8874; (b) M. A. AlDamen, S. Cardona-Serra, J. M. Clemente-Juan, E. Coronado, A. Gaita-Arinño, C. Martí-Gastaldo, F. Luis, O. Montero, *Inorg. Chem.* 2009, **48**, 3467.
24 S. D. Jiang, B. W. Wang, G. Su, Z. M. Wang, S. Gao, *Angew. Chem. Int. Ed.* 2010, **49**, 7448.
25 S. D. Jiang, B. W. Wang, H. L. Sun, Z. M. Wang, S. Gao, *J. Am. Chem. Soc*. 2011, **133**, 4730.
26 S. Cardona-Serra, J. M. Clemente-Juan, E. Coronado, A. Gaita-Ariño, A. Camón, M. Evangelisti, F. Luis, M. J. Martínez-Pérez, J. Sesé, *J. Am. Chem. Soc*. 2012, **134**, 14982.
27 D. E. Freedman, W. H. Harman, T. D. Harris, G. J. Long, C. J. Chang, J. R. Long, *J. Am. Chem. Soc.* 2010, **132**, 1224.
28 J. D. Rinehart, J. R. Long, *J. Am. Chem. Soc.* 2009, *131*, 12558.
29 L. R. Melby, N. J. Rose, E. Abramson and J. C. Caris, *J. Am. Chem. Soc.* 1964, **86**, 5117.
30 S. Alvarez, P. Alemany, D. Casanova, J. Cirera, M. Llunell, D. Avnir, *Coord. Chem. Rev*. 2005, **249**, 1693.
31 J. Cirera, E. Ruiz and S. Alvarez, *Organometallics*, 2005, *24*, 1556.
32 P. E. Car, M. Perfetti, M. Mannini, A. Favre, A. Caneschi, R. Sessoli, *Chem. Commun*. 2011, **47**, 3751.
33 A. Watanabe, A. Yamashita, M. Nakano, T. Yamamura,T. Kajiwara, *Chem. Eur. J*. 2011, **17**, 7428.
34 M. Jeletic, P. H. Lin, J. J. Le Roy, I. Korobkov, S. I. Gorelsky, M. Murugesu, *J. Am. Chem. Soc.* 2011, **133**, 19286.
35 J. Ruiz, A. J. Mota, A. Rodríguez-Diéguez, S. Titos, J. M. Herrera, E. Ruiz, E. Cremades, J. P. Costes, E. Colacio, *Chem. Commun*. 2012, **48**, 7916.
36 F. R. Fortea-Pérez, J. Vallejo, M. Julve, F. Lloret, G. De Munno, D. Armentano, E.Pardo *Inorg. Chem.* 2013, **52**, 4777.
37 P. Martín-Ramos, M. R. Silva, J. T. Coutinho, L. C. J. Pereira, P. Chamorro-Posada, J. Martín-Gil, *Eur. J. Inorg. Chem.* 2014, 511.
38 S. D. Jiang, S. S. Liu, L. N. Zhou, B. W. Wang, Z. M. Wang, S. Gao, *Inorg. Chem.* 2012, **51**, 3079.
39 J. D. Rinehart, K. R. Meihaus, J. R. Long, *J. Am. Chem. Soc.* 2010, **132**, 7572.
40 G. Cucinotta, M. Perfetti, J. Luzon, M. Etienne, P. E. Car, A. Caneschi, G. Calvez, K. Bernot, R. Sessoli, *Angew. Chem. Int. Ed.* 2012, **51**, 1606.
41 G. Cosquer, F. Pointillart, S. Golhen, O. Cador, L. Ouahab, *Chem. Eur. J*. 2013, **19**, 7895.
42 H. Bauer, J. Blanc, D. L. Ross, *J. Am. Chem. Soc.* 1964, **86**, 5125.
43 (a) Sheldrick, G. M. SHELXS-97, Program for X-ray Crystal Structure Solution, University of Göttingen, Germany, 1997. (b) Sheldrick, G. M. SHELXL-97, Program for X-ray Crystal Structure Refinement, University of Göttingen, Germany, 1997.
44 G. Karlström, R. Lindh, P. –Å. Malmqvist, B. O. Roos, U. Ryde, V. Veryazov, P. -O. Widmark, M. Cossi, B. Schimmelpfennig, P. Neogrady, L. Seijo, MOLCAS: a Program Package for Computational Chemistry. *Comput. Mater. Sci.* 2003, **28**, 222.

